Journal of Evolving Space Activities
Vol. 2, Article No. 149, 2024
DOI: 10.57350/jesa.149
Research Note

Evaluation of Grooved Needle Emitter Performance for Ionic Liquid Electrospray Thrusters

By Koki MATSUKAWA[1)] and Yoshinori TAKAO[2)]

[1)]*Department of Mechanical Engineering, Materials Science, and Ocean Engineering, Yokohama National University, Yokohama, Japan*
[2)]*Division of Systems Research, Yokohama National University, Yokohama, Japan*

(Received August 28th, 2023)

We have fabricated an externally wetted emitter array with a deep-grooved structure using grayscale lithography for ionic liquid electrospray thrusters to improve the ionic liquid transport to the emitter tips and to reduce the percentage of the current intercepted by the extractor electrode, which was more than 30% with our conventional deep-grooved emitter. The experimental results of the ion emission have shown that a stable ion emission characteristic and the percentage of the current intercepted by the extractor electrode decreases by approximately one-third compared with our previous one. This decrease indicates that the emitter fabrication process using grayscale lithography optimized the deep-grooved emitter shape.

Key Words: Electric Propulsion, Electrospray, Grooved Needle Emitter, Ionic Liquid, Grayscale Lithography

1. Introduction

In recent years, various advanced space missions that require precise control of the spacecraft's attitude and position have been proposed. For example, space gravitational wave observatories are currently under development to detect low-frequency gravitational waves that cannot be detected on Earth. The LISA mission by NASA and ESA will detect picometer-level changes due to the gravitational waves in the arm lengths between three spacecraft located 2.5 million kilometers apart.[1,2)] Therefore, such a mission requires a thruster with precise thrust control.[3)]

Ionic liquid electrospray thrusters have attracted attention as electric propulsion systems that can precisely control the thrust.[4-6)] Figure 1 shows a schematic of an electrospray thruster. Electrospray thrusters are composed of an emitter chip with many emitters on its surface and an opposing extractor electrode. When high voltages of several kilovolts between the emitters and extractor electrodes are applied, the ionic liquid is transported to the emitter tips, and ions are extracted due to the strong electric field. Then, the extracted ions are accelerated electrostatically by the electric potential difference between the two electrodes and generate thrust.

Ionic liquids are molten salts consisting only of cations and anions, and they have almost zero vapor pressure owing to the Coulomb force between the cations and anions.[7,8)] Therefore, ionic liquids can exist as a liquid phase even in vacuum, eliminating the need for high-pressure gas feed systems, including gas valves with their mechanical vibration required for conventional electric propulsion. Moreover, electrospray thrusters can extract both cations and anions by changing the polarity of the applied voltage, eliminating the need for neutralizers. In addition, the thrust can be controlled precisely by adjusting the number of emitters and the voltage applied to the emitters due to only a small amount of thrust on the order of 10 nN in the pure-ion mode per emitter.[9)]

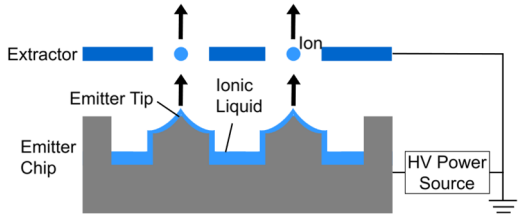

Fig. 1. Schematic of the electrospray thrusters. Modified illustration based on the original figure from Ref. 10), under CC BY 4.0 license. This modified figure is licensed under a Creative Commons Attribution 4.0 International License. Changes made include color adjustments and annotations.

For precise thrust control, it is necessary to extract a stable ion current from the emitter array. In our previous study, we fabricated externally wetted needle-shaped emitters with a deep-grooved structure.[10)] Compared with non-grooved needle emitters,[11)] the resulting absolute emission current value with the deep-grooved needle was approximately 30 times larger, and the current-voltage characteristics indicated a stable ionic liquid supply to the emitter tips. However, more than 30% of the current was intercepted by the extractor electrode through deep grooving. This is probably due to the electric field concentrated on both emitter tips and protuberances on the emitter sides. To decrease the extractor current, we have fabricated deep-grooved emitters using grayscale lithography and have evaluated the characteristics of the resulting ion beam. This paper reports the results of the emitter fabrication and ion emission experiments.

2. Fabrication of the Emitter Chip

We have fabricated the emitter chip with an array of grooved needle emitters by using the technique to fabricate micro-electro-mechanical-system (MEMS) devices. In order to prevent an increasing percentage of the current intercepted by the extractor electrode for deep-grooved emitters, the protuberances on the emitter sides should be removed or close to the emitter bottom so that the electric field is concentrated only.

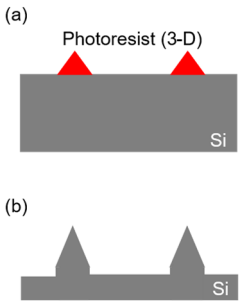

Fig. 2. Fabrication process of the emitters.

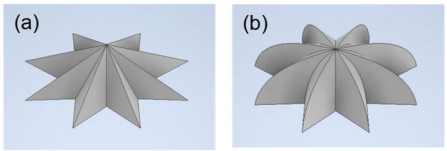

Fig. 3. Schematic of the etching mask for the grayscale photolithography: (a) Cone-shaped and (b) domed mask.

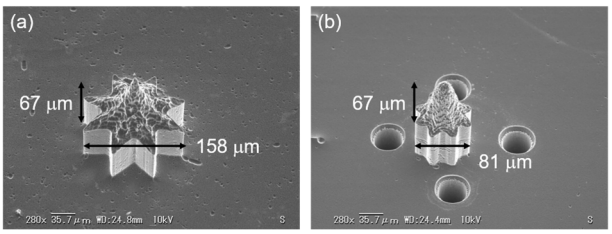

Fig. 4. SEM images of the grooved emitter using (a) cone-shaped and (b) domed mask.

on the emitter tips.

We employed a fabrication process using grayscale photolithography to obtain the shape of the deep-grooved emitter without the protuberances on the emitter sides. Grayscale photolithography is a microfabrication technique for creating three-dimensional (3-D) microstructures in photoresist.[12,13] Figure 2 shows the fabrication steps of the emitters using grayscale photolithography. First, a photoresist was coated on the surface of a 4-inch silicon wafer, and grayscale photolithography was conducted. After development, 3-D microstructures remained as etching masks [Fig. 2(a)]. Then, the mask shape is transferred to the silicon by anisotropic etching using the Bosch process while etching the 3-D etching mask [Fig. 2(b)].[14] Figure 3 shows a schematic of the 3-D etching masks. We used two types of 3-D etching mask shapes: a cone-shaped mask with an outer diameter of 200 μm and a groove depth of 50 μm [Fig. 3(a)], and a domed mask with an outer diameter of 100 μm and a groove depth of 25 μm [Fig. 3(b)]. For the deep-grooved emitter shape, a large mask diameter may increase the percentage of the current intercepted by the extractor electrode due to the protuberances on the emitter sides; thus, we also employed an outer diameter of 100 μm for the domed mask. In this study, the emitter chip has a 9×9 array of 81 grooved emitters.

Figure 4(a) shows an SEM image of one of the fabricated grooved emitters using the cone-shaped mask. The distance between the emitter tip and protuberances on the emitter side

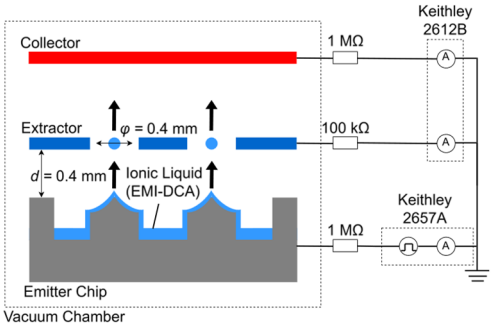

Fig. 5. Schematic of the experimental setup for the ion current measurements without an ionic liquid supply system. Modified illustration based on the original figure from Ref. 10), under CC BY 4.0 license. This modified figure is licensed under a Creative Commons Attribution 4.0 International License. Changes made include color adjustments and annotations.

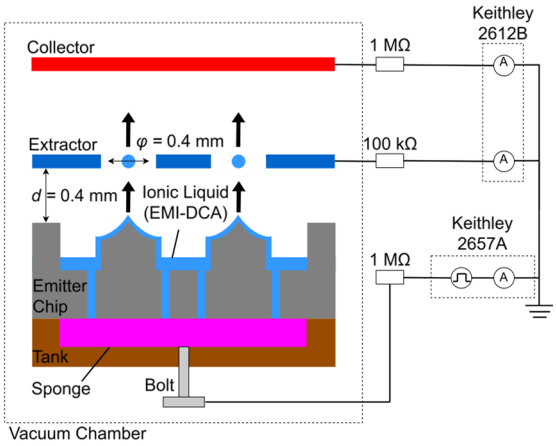

Fig. 6. Schematic of the experimental setup for the ion current measurements supplying ionic liquid from the back side of the emitter chip. Modified illustration based on the original figure from Ref. 10), under CC BY 4.0 license. This modified figure is licensed under a Creative Commons Attribution 4.0 International License. Changes made include color adjustments and annotations.

was 67 μm, which is larger than that of our previous grooved emitter [23 μm: see Fig. 4(c) or Fig. 20(a) in Ref. 10)]. This increased distance leads to an increase in the distance between the protuberances on the emitter side and the extractor. However, the mask shape was not completely transferred to the silicon wafer, and the protuberances on the emitter sides remained probably because the photoresist etching had not progressed immediately after the start of the etching.

Figure 4(b) shows an SEM image of one of the fabricated grooved emitters using the domed mask. We achieved an emitter shape with a gently sloping ridge from the emitter sides to the emitter tip that appears to reduce the electric field's concentration on the protuberances of the emitter sides by using the domed and small diameter mask. The slope angle of the ridge was approximately 50 degrees while that was approximately 17 degrees with the grooved emitter using the cone-shaped mask. Notably, the four through holes at the emitter base are an ionic liquid supply system to supply ionic liquid from the back side of the emitter chip. The fabrication process of the ionic liquid supply system is the same as that in our previous paper [see Fig. 5 in Ref. 10)].

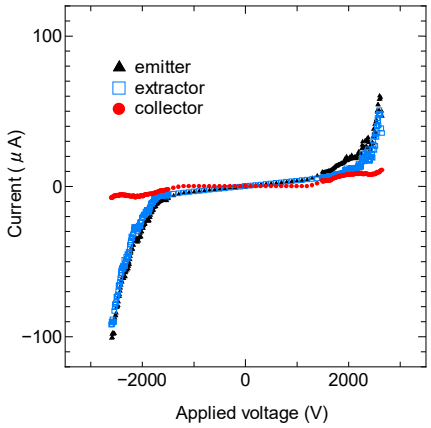

Fig. 7. Current-voltage characteristics of 81-grooved emitters fabricated using the cone-shaped mask.

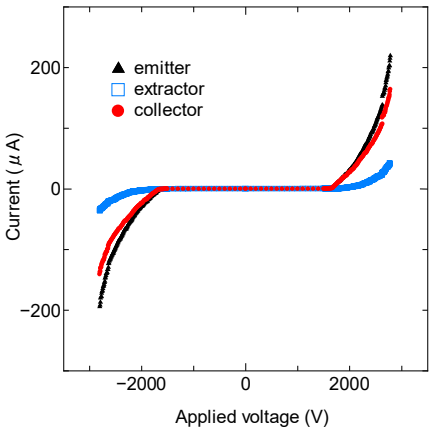

Fig. 8. Current-voltage characteristics of 81-grooved emitters fabricated using the domed mask.

3. Ion Emission Experiment

Figure 5 shows the experimental setup for measuring the ion emission current. This setup is the same as that in our previous study.[10] The distance between the emitter chip and the extractor electrode was set at d = 0.4 mm, and the extractor electrode had an aperture of φ = 0.4 mm in diameter. The extractor electrode was fabricated by etching a silicon wafer.[11] The ion emission experiment was performed in a vacuum chamber at 2×10^{-3} Pa or less.

We used an ionic liquid of 1-ethyl-3-methylimidazolium dicyanamide (EMI-DCA) as a propellant. EMI-DCA is one of the propellant candidates for electrospray thrusters and tends to emit ions in the purely ionic regime. We supplied 0.01 μl of EMI-DCA by dropping it onto the emitter chip.

We applied a bipolar pulse voltage of 1 Hz to the emitter chip and measured the currents of the emitter using a source meter (Keithley 2657A) through a 1 MΩ resistor. The extractor and collector electrodes were set at 0 V by the source meter (Keithley 2612B) through 100 kΩ and 1 MΩ resistors, respectively. These resistors were for source meter protection. In ground testing, current measurements may become unreliable due to secondary species emissions (SSEs) caused by high-energy ions colliding against the chamber walls and collector surfaces.[15,16] However, we concentrated on the emitter and extractor currents using source meters, which can accurately measure the tiny DC currents of emitters at high voltages in this study. Therefore, the collector currents were treated as a reference, which we verified to be almost equal to the sum of the emitter and extractor currents.

Figure 6 shows the experimental setup for the emitter chip with an ionic liquid supply system. This experimental setup was almost the same as Fig. 5, but the ionic liquid was supplied from the tank of the backside of the emitter chip. We applied a bipolar pulse voltage of 1 Hz to the ionic liquid through the bolt and measured each current. The pore diameter of the sponge was much larger than the diameter of through holes, allowing ionic liquid to be supplied to the emitter passively by capillary phenomenon.

Figure 7 shows the results of the ion emission experiment with an array of 81-grooved emitters using the cone-shaped mask. The horizontal axis in Fig. 7 is the voltage applied to the emitter chip, considering the voltage drops across the 1 MΩ protection resistor. These results were obtained with the experimental setup shown in Fig. 5. As shown in Fig. 7, on the positive side, the maximum emitter currents were 60.2 μA at 2600 V, and on the negative side, the minimum emitter currents were −101 μA at −2599 V. Compared with the result of the previous grooved needle emitters, the absolute emission current significantly decreased, and the current-voltage characteristics tended to be unstable. These results may have been caused by the absence of the ionic liquid supply system resulting in an insufficient and unstable supply of ionic liquid. In addition, the percentage of the current intercepted by the extractor electrode did not decrease, but instead increased. This result is attributed to a larger diameter than the previous grooved emitter, which indicates that the electric field is still concentrated on the protuberances on the emitter sides.

Figure 8 shows the results of the ion emission experiment with an array of 81-grooved emitters using the domed mask. The horizontal axis in Fig. 8 is the voltage applied to the emitter chip, considering the voltage drops across the 1 MΩ protection resistor. These results were obtained with the experimental setup shown in Fig. 6. The maximum emitter currents were 220 μA at 2781 V, and the minimum emitter currents were −194 μA at −2806 V. Compared with non-grooved needle emitters, the absolute emission current value increased by more than 10 times.[11] In addition, the slope of the current-voltage curves did not decrease, indicating sufficient ionic liquid transport to the emitter tips. Moreover, the percentage of current interrupted by the extractor electrode was 10.7% at about 2200 V. The percentage decreased by approximately one-third compared with our previous deep-grooved emitter.[10] This decrease indicates the emitter fabrication process using the grayscale lithography optimized the shape of the deep-grooved emitter, and that this improved shape suppressed the concentration of the electric field on the protuberances on the emitter sides.

4. Conclusion

In this study, we have fabricated externally wetted needle-shaped emitters with a deep-grooved structure using grayscale lithography to suppress the concentration of the electric field on the protuberances on the emitter sides. Two types of grooved emitters with different shapes were successfully fabricated by changing the design of the etching mask. As the result of the current-voltage measurement with the emitters using the domed and small diameter etching mask, the emitter current reached 220 μA at 2781 V, and −194 μA at −2806 V. The percentage of current interrupted by the extractor electrode was 10.7% whereas the percentage was 30.3% with our previous deep-grooved emitters.[10] These results indicate that the deep-grooved emitter shape fabricated by grayscale lithography provides stable ionic liquid transport to the emitter tips and allows electric field concentration to occur only at the tips, suppressing ion current interruption at the extractor electrode. In the future, we will investigate the ion beam characteristics, such as the composition of the ion beam by time-of-flight measurements to estimate the thruster performance.

Acknowledgments

This work was partially supported by JSPS KAKENHI Grant No. JP21H01530, the Canon Foundation, the Advisory Committee for Space Engineering of Japan Aerospace Exploration Agency, and JST FOREST Program Grant No. JPMJFR2129. A part of this work was conducted at the Takeda Sentanchi Supercleanroom at the University of Tokyo, supported by "Advanced Research Infrastructure for Materials and Nanotechnology in Japan (ARIM)" of the Ministry of Education, Culture, Sports, Science and Technology (MEXT). (Proposal No. JPMXP1223UT1022). SEM observation was carried out by VE-8800, Instrumental Analysis Center at Yokohama National University.

References

1) Laser Interferometer Space Antenna, http://lisa.nasa.gov (accessed January 21, 2023).
2) Armano, M., Benedetti, M., Bogenstahl, J., Bortoluzzi, D., Bosetti, P., Brandt, N., et al.: LISA Pathfinder: the Experiment and the Route to LISA, *Class. Quantum Grav.*, **26** (2009), pp. 094001-1–16.
3) Scharlemann, C., Buldrini, N., Killinger, R., Jentsch, M., Polli, A., Ceruti, L., Serafini, D., and Nicolini, D.: Qualification Test Series of the Indium Needle FEEP Micro-Propulsion System for LISA Pathfinder, *Acta Astronaut.*, **69** (2011), pp. 822–832.
4) Lozano, P. and Martínez-Sánchez, M.: Ionic Liquid Ion Sources: Characterization of Externally Wetted Emitters, *J. Colloid Interface Sci.*, **282** (2005), pp. 415–421.
5) Hill, F. A., Heubel, E. V., Ponce de Leon, P., and Velasquez-Garcia, L. F.: High-Throughput Ionic Liquid Ion Sources Using Arrays of Microfabricated Electrospray Emitters with Integrated Extractor Grid and Carbon Nanotube Flow Control Structures, *J. Microelectromech. Syst*., **23** (2014), pp. 1237–1248.
6) Dandavino, S., Ataman, C., Ryan, C. N., Chakraborty, S., Courtney, D., Stark, J. P. W., et al.: Microfabricated Electrospray Emitter Arrays with Integrated Extractor and Accelerator Electrodes for the Propulsion of Small Spacecraft, *J. Micromech. Microeng.*, **24** (2014), pp. 075011-1–13.
7) Kitazawa, Y., Ueno, K., and Watanabe, M.: Advanced Materials Based on Polymers and Ionic Liquids, *Chem. Rec.*, **18** (2017), pp. 391–409.
8) Nishikawa, K.: General Remarks on Ionic Liquids, Which Are Applicable under Vacuum, *J. Vac. Soc. Japan*., **56** (2013), pp. 43–46 (in Japanese).
9) Petro, E., Bruno, A., Lozano, P., Perna L. E., and Freeman, D.: Characterization of the TILE Electrospray Emitters, AIAA Paper 2020-3612, 2020.
10) Matsukawa, K., Nakashima, Y., Naemura, M., and Takao, Y.: Emission Measurements and in-situ Observation of Ionic Liquid Electrospray Thrusters with Longitudinally Grooved Emitters, *J. Electr. Propuls*,**2** (2023).
11) Tachibana, F., Tsuchiya, T., and Takao. Y.: Uniform Needle-Emitter Arrays for Ionic Liquid Electrospray Thrusters with Precise Thrust Control, *Jpn. J. Appl. Phys.*, **60** (2021), pp. SCCL06-1–9.
12) Smith, M. A., Berry, S., Parameswaran, L., Holtsberg, C., Siegel, N., Lockwood, R., et al.: Design, Simulation, and Fabrication of Three-Dimensional Microsystem Components Using Grayscale Photolithography, *J. Micro/Nanolith. MEMS MOEMS.,* **18** (2019), pp. 043507-1–14.
13) Corrado, M. N., Lozano, P. C., Parameswaran, L., Cook, M., Holihan, E. C., Mathews, R., et al.: Densification of Ionic Liquid Electrospray Thrusters Using Silicon-Based MEMS Fabrication, 37th International Electric Propulsion Conference, Boston, USA, IEPC-2022-177, 2022.
14) Roozeboom, F., van den Bruele, F., Creyghton, Y., Poodt, P., and Kessels, W. M. M.: Cyclic Etch/Passivation-Deposition as an All-Spatial Concept toward High-Rate Room Temperature Atomic Layer Etching, *ECS J. Solid State Sci. Technol*., **4** (2015), pp. N5067–N5076.
15) Uchizono, N. M., Collins, A. L., Marrese-Reading, C., Arestie, S. M., Ziemer, J. K., and Wirz, R. E.: The Role of Secondary Species Emission in Vacuum Facility Effects for Electrospray Thrusters, *J. Appl. Phys.*, **130** (2021), pp. 143301-1–21.
16) Klosterman, M. R., Rovey, J. L., and Levin, D. A.: Ion-induced charge emission from unpolished surfaces bombarded by an [Emim][BF_4] electrospray plume, *J. Appl. Phys.*, **131** (2022), pp. 243302-1–17.